

Article

Low-Temperature Performance of Asphalt Mixtures Modified by Microencapsulated Phase Change Materials with Various Graphene Contents

Yong-Xiang Ren ^{1,2} and Pei-Wen Hao ^{1,*}¹ School of Highway, Chang'an University, Xi'an 710064, China; renyx@chd.edu.cn² Xuchang Vocational and Technical College, Xuchang 461000, China

* Correspondence: pwhao@chd.edu.cn

Abstract: Microencapsulated phase change materials (PCMs) added to conventional ones can store excessive heat energy and reduce thermal stresses. In this study, melamine–formaldehyde resin phase change microencapsulated PCMs, with different contents of graphene (CG), were added to asphalt mixtures, in order to reduce their low-temperature cracking, induced by thermal stresses. Low-temperature and heat-conducting/storing performance of the obtained mixtures was examined via beam bending tests, semi-circular bending low-temperature performance tests, thermal conductivity tests and volume-specific heat capacity tests. Besides, the prepared asphalt mixtures' water stability and high-temperature stability values were obtained via freeze-thaw splitting and wheel tracking tests. The low-temperature performance of PCM-modified asphalt mixtures was evaluated via their bending strain energy densities, with one of the PCM-modified asphalt mixtures, namely CGMFPCM3, synthesized by the authors, was 1.7 times higher than that of the common asphalt mixture. Although the dynamic stability of all three PCM-modified mixtures was deteriorated by 68, 50, and 20% compared to the common one, that of CGMFPCM3 still complied with the standard requirement. Thermal conductivity and volume-specific heat capacity of the asphalt mixture at 278.15 K was enhanced by 5 and 43%, respectively, after adding CGMFPCM3. It is recommended for reducing the temperature variation-induced cracking in the asphalt pavement. Thermal conductivity and volume-specific heat capacity can be used for evaluating the temperature-regulating performance of asphalt mixtures.

Keywords: graphene; phase change materials; asphalt mixture; low-temperature performance; temperature-regulating performance



Citation: Ren, Y.-X.; Hao, P.-W. Low-Temperature Performance of Asphalt Mixtures Modified by Microencapsulated Phase Change Materials with Various Graphene Contents. *Coatings* **2022**, *12*, 287. <https://doi.org/10.3390/coatings12020287>

Academic Editors: Qiao Dong and Andrea Simone

Received: 12 January 2022

Accepted: 16 February 2022

Published: 21 February 2022

Publisher's Note: MDPI stays neutral with regard to jurisdictional claims in published maps and institutional affiliations.



Copyright: © 2022 by the authors. Licensee MDPI, Basel, Switzerland. This article is an open access article distributed under the terms and conditions of the Creative Commons Attribution (CC BY) license (<https://creativecommons.org/licenses/by/4.0/>).

1. Introduction

The mechanical and physical properties of asphalt and its mixtures strongly depend on temperature variations. Under ambient temperature conditions, thermal stresses in the pavement induced by temperature variation are gradually relaxed, due to the viscoelastic behavior of asphalt. However, at a certain level of low climatic temperatures, asphalt's stress–strain state changes from viscoelastic to purely elastic, inhibiting the relaxation of thermal stresses and promoting the asphalt mixture cracking, as soon as thermal stresses exceed the asphalt's tensile strength limit [1].

Special phase change materials (PCMs) have been introduced to absorb or release the latent heat during the phase change process to achieve high- or low-temperature adjustment, thereby exhibiting great potential in reducing the temperature variation-induced cracks on the bituminous pavement surface. However, some test results revealed that the direct addition of PCMs to an asphalt matrix can deteriorate the technological performance of modified asphalt [2–4] or modified asphalt mixtures [5–8], due to poor bonding between PCMs and the material matrix. This problem has been mitigated by encapsulation of PCMs via some phase-change micro-capsulation technologies, namely the physical adsorption

film coating [9–12], interfacial polymerization [13–15], and in-situ polymerization [16–23], minimizing the direct contact between PCM and asphalt. Different kinds of phase change microcapsules have significant effects on the technical properties of phase change modified asphalt and mixtures. It is found that phase change microcapsules can improve the performance of asphalt [24], but the performance of the phase change modified asphalt mixture is reduced [20].

Currently, the low-temperature performance of asphalt mixtures is evaluated by the test methods regulated by international and national standards, including the D-type compressive tensile tests via ASTM D7313 [25], indirect tensile tests via AASHTO T322 [26], semi-circular bending (SCB) tests via AASHTO TP105 [27], low-temperature confining tests via EN 12697-44 [28] and AASHTO TP10 [29], and the evaluation method for the cracking resistance of asphalt mixtures at low temperatures via GB/T 38948-2020 [30]. AC-13 semi-circular bending (SCB) loading test results on pavement core samples demonstrate a strong correlation between fracture energy indexes and the actual cracking performance of bituminous pavement [31]. According to the calculation formula of temperature stress, proposed by hills [32], under the same external temperature change conditions, the temperature stress of an asphalt mixture is consistent with the change trend of the stiffness modulus of the mixture itself. The evaluation method of low temperature crack resistance of the asphalt mixture (GB/T 38948-2020) [30] proposes that the bending strain energy density is used to evaluate the low temperature crack resistance of the asphalt mixture. The temperature-regulating performance of phase change modified bituminous pavement is generally evaluated using the following three methods: finite element modeling [33,34], indoor and outdoor real-time monitoring [3,35–37], and the measurement of such thermal parameters as thermal conductivity and specific heat capacity [38–40]. In finite element modeling, the material properties should be pre-defined, while indoor and outdoor real-time monitoring should be performed under specific environments. Thermal conductivity is an inherent material attribute, reflecting the overall heat-conducting performance of a phase change-modified asphalt mixture. Specific heat capacity characterizes the capability of the material to enhance the temperature, rather than absorbing or dissipating heat. Since the samples used in the specific heat capacity test are usually quite small and have small mass, the laboratory test results for asphalt mixtures have low reliability for large-scale asphalt pavements due to the size effect. In contrast, volumetric specific heat capacity measures the relation between the heat energy of material and temperature in a unit volume, which can more appropriately reflect the effect of added PCMs on the heat storage performance of asphalt mixtures. Therefore, it is very necessary to study the evaluation methods of low-temperature performance and temperature regulation performance of a phase change modified asphalt mixture.

Molecular simulation and indoor test research show that the road performance of a modified asphalt mixture, prepared with graphene (CG) modified asphalt, will be enhanced [41–43], and the phase change energy storage and release efficiency of CG composite phase change microcapsules is also greatly improved, compared with ordinary phase change microcapsules [44]. Therefore, in order to further study the technical performance of a graphene reinforced phase change temperature regulating asphalt mixture, three kinds of phase change modified asphalt mixtures were prepared by using self-made graphene composite melamine formaldehyde resin phase change microcapsules (CGMFPCM), with different CG content (0, 0.3 and 0.45%). Low-temperature performance was evaluated via beam bending tests and semi-circular bending (SCB) tests, via AASHTO TP105 [27]. Heat conduction/storage performances were evaluated by the thermal conductivity and volume-specific heat capacity tests. Finally, water stability and high-temperature stability of the phase change-modified asphalt mixtures were validated via freeze–thaw slitting and wheel tracking tests.

2. Materials and Methods

2.1. Test Materials

2.1.1. Matrix Asphalt

The 70# matrix asphalt manufactured by the Shandong Kelida Company, Shandong, China, was used in this study, with technical properties listed in Table 1.

Table 1. Technical properties of the matrix asphalt.

Technical Properties	Test Result	Specification Limits	Standard in China (JTG E20-2011)
Penetration (25 °C, 0.1 mm)	77.9	60–80	T0604-2011
Softening point (°C)	46	≥46	T0606-2011
Dynamic viscosity (60 °C, Pa·s)	240	≥180	T0620-2000
Penetration index	−1.24	−1.5~+1.0	T0604-2011
Density (15 °C, g/cm ³)	1.023	—	T0603-2011
Solution (Chloral, %)	99.95	≥99.5	T0607-2011
Flash point(°C)	300	≥260	T0611-2011
Ductility (10 °C, cm)	40.5	≥25	T0605-2011
Ductility (15 °C, cm)	>100	≥100	T0605-2011
Wax content (Distillation, %)	1.1	≤2.2	T0615-2011

2.1.2. Phase Change Microcapsules

In this study, the previously prepared MFPCM, CGMFPCM2 and CGMFPCM3 phase change microcapsules [43] were selected, and the technical indexes are shown in Table 2.

Table 2. Technical specifications of phase change microcapsules.

Type	Phase Transition Temperature/°C	Latent Heat/kJ·kg ^{−1}	Content of CG in Microcapsule Wall Material/%
MFPCM	3.05~6.61	26.89	—
CGMFPCM2	4.07~6.73	99.90	0.30
CGMFPCM3	2.12~5.85	9.09	0.45

2.1.3. Asphalt Mixture

Using MFPCM, CGMFPCM2, and CGMFPCM3 as modifiers, three different modified asphalt mixture specimens were prepared via high-speed shearing, in which the mix ratio of the modifier was fixed at 5% [43]. Next, by selecting basalt and limestone as coarse and fine aggregates, based on the mix proportion design method of hot mix asphalt mixture in Technical Specification for Construction of Highway Asphalt Pavements (JTG F40-2004) [45], respectively, common asphalt and three different modified asphalt mixtures were prepared with limestone mineral powder and AC-16 grading bitumen. Table 3 lists the passing rates of the mixtures at different grades. The optimal asphalt-aggregate (percentage to total mineral aggregate) of the asphalt mixture was determined by the Marshall test, and the results obtained are listed in Table 4.

Table 3. The passing rate of each sieve of the mixture's grade.

Sieve/mm	19	16	13.2	9.5	4.75	2.36	1.18	0.6	0.3	0.15	0.075
Passing rate/%	100	94.4	83.8	72.8	49.4	36.1	30.3	18.4	9.6	6.7	5.7

Table 4. Optimal asphalt-aggregate of the AC-16 bitumen.

Type of Asphalt	Optimal Asphalt-Aggregate Ratio/%	Gross Volume Relative Density	Void Ratio/%	Void Ratio of Mineral Aggregate/%	Saturation Degree of Asphalt/%
Matrix asphalt	4.5	2.490	4.0	13.3	70.0
MFPCM	4.5	2.495	4.0	13.4	69.8
CGMFPCM2	4.5	2.519	3.5	12.9	72.8
CGMFPCM3	4.5	2.495	4.0	13.3	69.8

2.2. Test Methods

2.2.1. Low-Temperature Performance Test (SCB Method)

With reference to the AASHTO TP105 method [27], semi-circular bending (SCB) tests were performed. Cylindrical specimens with a diameter of 101.6 mm and a height of 63.5 mm were prepared according to the T0702-2011 method [46], which were then cut into the semi-circular specimens with a thickness of 25 mm and a fracture depth of 10 mm on the numerical-controlled machine tool. Figure 1 shows specimens from different materials used in the low-temperature test (SCB test).



Figure 1. Specimens under low-temperature performance test (SCB test): (a) common asphalt mixture, (b) MFPCM-modified asphalt mixture, (c) CGMFPCM2-modified asphalt mixture and (d) CGMFPCM3-modified asphalt mixture.

Next, the asphalt mixture's low-temperature crack resistance tests were performed via an electro-hydraulic servo universal material tester (MTS). The loading rate and span were fixed at 1 mm/s min, 80 mm, respectively. The test temperatures were $-20\text{ }^{\circ}\text{C}$ and $-10\text{ }^{\circ}\text{C}$, respectively, and the parallel test was conducted for 3 times. The fracture energy G_f , the fracture toughness K_{IC} and the stiffness S were then calculated to evaluate crack resistance performance.

The fracture energy G_f is the ratio between the work on fracture (the area between load and mean displacement under load) and the ductile zone area, shown in the following equation:

$$G_f = \frac{W_f}{A_{lig}} \quad (1)$$

where G_f is the fracture energy (in J/m^2), A_{lig} is the ductile zone area (in m^2), and W_f is the work on fracture (in J). The latter two parameters are derived as follows: $W_f = \int Pdu$, where P is the applied load, (in N), and u is the mean displacement under load (in m); $A_{lig} = (r - a) \times t$, where r is the specimen radius (in m), a is the incision length, and t is the specimen thickness.

The fracture toughness K_{IC} can be calculated as follows:

$$K_{IC} = Y_{I(0.8)} \times \sigma_0 \times \sqrt{\pi a} \quad (2)$$

where $\sigma_0 = \frac{P}{2rt}$; $Y_{I(0.8)}$ is the standard stress intensity factor (a dimensionless unit); $Y_{I(0.8)} = 4.782 + 1.219\left(\frac{a}{r}\right) + 0.063 \exp\left(7.045\left(\frac{a}{r}\right)\right)$.

The stiffness S can be obtained by calculating the slope of the load-mean displacement (P - u) curve in the ascent stage, with a unit of KN/mm .

2.2.2. Bending Tests

According to the T0715-2011 method [47], after grinding wheel molding of asphalt mixture, plate specimens were cut into prismoid-shaped beams with a length of 250 mm, a width of 30 mm, and a height of 35 mm. The mechanical properties were then tested via an electro-hydraulic servo universal material tester (MTS). The loading rate, span, and temperature were fixed at 50 mm/s min, 200 mm, and $-10\text{ }^{\circ}\text{C}$, respectively. Parallel test was conducted 6 times. Next, the specimen flexural strength R_B , the maximum flexural-tensile strain ε_B , and the bending stiffness modulus S_B at the moment of failure were calculated via the following equations:

$$R_B = \frac{3 \times L \times P_B}{2 \times b \times h^2} \quad (3)$$

$$\varepsilon_B = \frac{6 \times h \times d}{L^2} \quad (4)$$

$$S_B = \frac{R_B}{\varepsilon_B} \quad (5)$$

where B and h are the specimen's width and height, respectively, at the mid-span section (in mm), L is the specimen span (in mm), P_B is the maximum load at failure (in N), and d is the mid-span deflection at failure (in mm).

Based on the GB/T 38948-2020 method [30], the bending strain energy density of the specimen, denoted as $\frac{dW}{dV}$, can be calculated according to the following equation:

$$\frac{dW}{dV} = \int_0^{\varepsilon_0} \sigma d\varepsilon = \int_0^{\varepsilon_0} f(\varepsilon) d\varepsilon \quad (6)$$

where $\frac{dW}{dV}$ is the bending strain energy density of the asphalt mixture (in KJ/m^3), ε_0 is the strain corresponding to the maximum stress at failure (in $\mu\varepsilon$), ε is the flexural-tensile strain at the beam bottom (in $\mu\varepsilon$), and σ is the stress at the beam bottom (in MPa).

2.2.3. Freeze–Thaw Splitting Test

According to the method described in T0729-2000 [48], freeze–thaw cyclic tests were performed on the cylindrical specimens of asphalt mixture via the Marshall compaction method (T0702-2011) [46] for measuring the strength ratio in splitting failure test before and after water damage and further evaluating water stability of asphalt mixture. The temperature and the loading rate were set at $25\text{ }^{\circ}\text{C}$ and 50 mm/min during the test, respectively, with 5 parallel tests.

2.2.4. Wheel Tracking Test

The standard wheel track plates with a size of $300\text{ mm} \times 300\text{ mm} \times 50\text{ mm}$ were prepared according to the method described in T0703-2011 [49]. The tests were conducted at a test temperature of $60\text{ }^{\circ}\text{C}$ and a wheel pressure of 0.7 MPa, with 3 parallel tests. The high-temperature stability of the asphalt mixture was evaluated via its dynamic stability.

2.2.5. Test of Thermal Conductivity and Volume-Specific Heat Capacity

Using the numerically-controlled machine tool, each of the cylindrical specimens with a diameter of 101.6 mm and a height of 63.5 mm prepared via the Marshall compaction method [46] were cut into two specimens with a length of 50 mm, a width of 50 mm and a thickness of 30 mm, as shown in Figure 2a–d. The thermal conductivities and volume-specific heat capacities of common and modified asphalt mixture specimens were measured by the TC5000E conductometer (manufactured by the Xi'an Xia'xi Electronic Science and Technology Company, China), In the temperature range of $-268.15\text{--}298.15\text{ K}$, at temperature intervals of 10 K, with parallel tests twice.

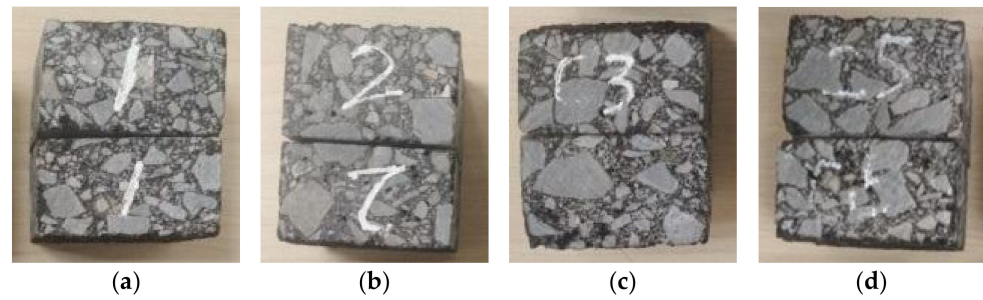


Figure 2. Specimens for the thermal conductivity and volume-specific heat capacity tests: (a) common asphalt mixture, (b) MFPCM-modified asphalt mixture, (c) CGMFPCM2-modified asphalt mixture, and (d) CGMFPCM3-modified asphalt mixture.

3. Results and Discussion

3.1. Low-Temperature Performance Test

3.1.1. Semi-Circular Bending Low-Temperature Performance Test

(1) Test results

Using low-temperature performance tests of the asphalt mixture, via the SCB method described in Section 2.2.1, the fracture energy G_f , the fracture toughness K_{IC} and the stiffness S were measured for evaluating the low-temperature crack resistance of asphalt mixtures. The test temperature was set at $-20\text{ }^\circ\text{C}$ and $-10\text{ }^\circ\text{C}$, respectively. Figures 3 and 4 show the test results.

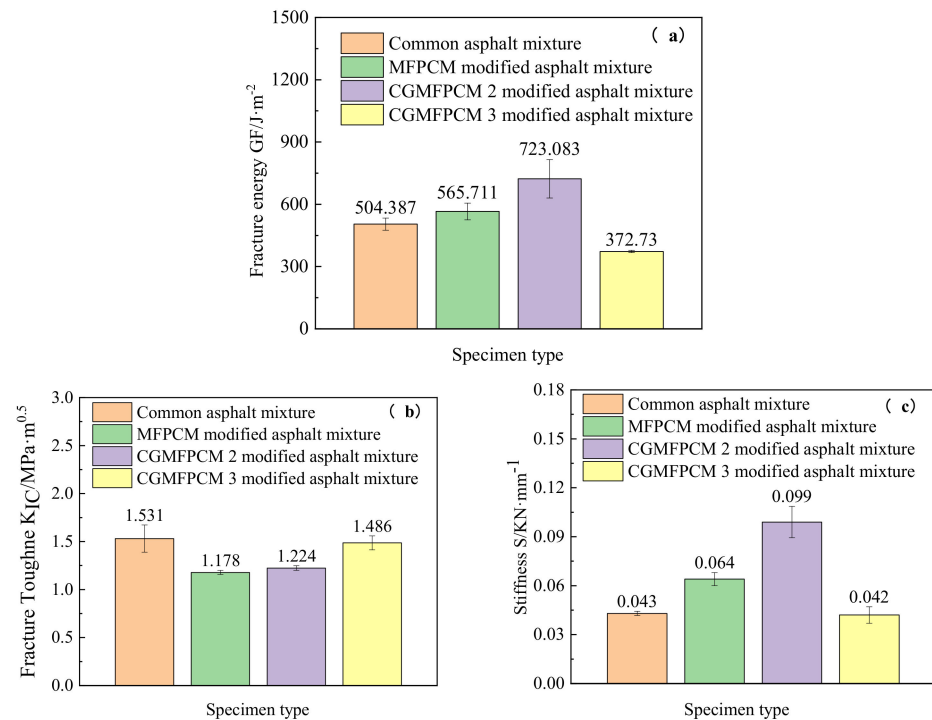


Figure 3. SCB test ($-20\text{ }^\circ\text{C}$) results for common and modified asphalt mixtures: (a) the fracture energy G_f , (b) the fracture toughness K_{IC} and (c) the stiffness S .

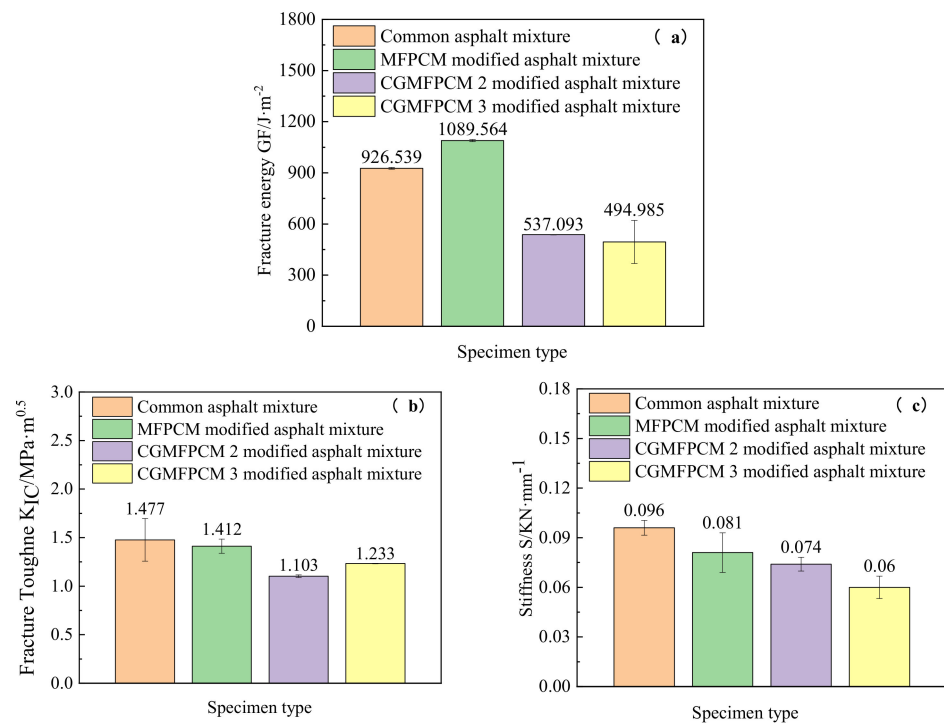


Figure 4. SCB test ($-10\text{ }^{\circ}\text{C}$) results for common and modified asphalt mixtures: (a) the fracture energy G_f , (b) the fracture toughness K_{IC} and (c) the stiffness S .

A larger fracture energy implies a better crack resistance performance. As shown in Figure 3a, after the addition of MFPCM and CGMFPCM2, the fracture energy of the asphalt mixture at a temperature of $-20\text{ }^{\circ}\text{C}$ was enhanced, as compared to that of the common asphalt mixture. In contrast, the fracture energy of the CGMFPCM3-modified asphalt mixture was reduced. The fracture energy value obtained in this test is basically consistent with the reported results of the pavement core sample $-20\text{ }^{\circ}\text{C}$ SCB test [31]. As shown in Figure 4a, after the addition of MFPCM, the fracture energy of the asphalt mixture at a temperature of $-10\text{ }^{\circ}\text{C}$ was enhanced, as compared to that of the common asphalt mixture. In contrast, the fracture energy of the CGMFPCM-modified asphalt mixture was reduced. According to the test results, it can be concluded that the low-temperature crack resistance performance of the asphalt mixture is enhanced after adding phase-change materials MFPCM, but deteriorated after adding CGMFPCM3.

The fracture toughness can reflect the material's ability to absorb energy during the fracturing process. A larger value of fracture toughness indicates a stronger capability of the specimen in preventing crack growth. As shown in Figures 3b and 4b, compared with common asphalt mixtures, the fracture toughness decreased after adding MFPCM, CGMFPCM2, and CGMFPCM3. The fracture toughness test results revealed that the addition of MFPCM, CGMFPCM2, and CGMFPCM3 could also deteriorate the low-temperature crack resistance performance of the asphalt mixture, to varying degrees. Moreover, the addition of CGMFPCM3 imposed a lesser effect on low-temperature crack resistance performance of the asphalt mixture.

The stiffness reflects the material's difficulty of elastic deformation. A smaller stiffness suggests a stronger ability of the specimen to resist crack propagation. As shown in Figure 3c, compared with the common asphalt mixture, the stiffness increased at $-20\text{ }^{\circ}\text{C}$, after adding MFPCM and CGMFPCM2, but dropped after adding CGMFPCM3. Conclusively, at $-20\text{ }^{\circ}\text{C}$, the addition of MFPCM and CGMFPCM2 harmed the low-temperature crack resistance performance of the asphalt mixture to a certain degree, while the addition of CGMFPCM3 imposed only a slight effect on it. As shown in Figure 4c, compared with the common asphalt mixture, the stiffness decreased at $-10\text{ }^{\circ}\text{C}$, after adding MFPCM, CGMFPCM2 and CGMFPCM3. The stiffness of the CGMFPCM3-modified asphalt mix-

ture was reduced to 62.5% of that of the ordinary asphalt mixture, indicating that the low-temperature crack resistance is enhanced. According to the test results, under different temperature conditions, it is concluded that CGMFPCM3 is helpful to enhance the low-temperature crack resistance of an asphalt mixture.

(2) Variance analysis

Tables 5–7 present variance analysis and significance results of the obtained SCB test data.

Table 5. Variance analysis of the fracture energy results in the performed SCB tests.

Temperature	Source of Variance	Sum of Squares	Degrees of Freedom	Mean Square Error	F	F _{0.05}
−20 °C	Graphene content in the PCM microcapsules	199,978.099	2	99,989.049	0.32	9.55
	Error	924,428.746	3	308,142.915		
	Sum	1,124,406.844	5			
−10 °C	Graphene content in the PCM microcapsules	36,033.046	2	18,016.523	0.03	9.55
	Error	2,036,094.788	3	678,698.263		
	Sum	2,072,127.834	5			

Table 6. Variance analysis of the fracture toughness results in the present SCB test.

Temperature	Source of Variance	Sum of Squares	Degrees of Freedom	Mean Square Error	F	F _{0.05}
−20 °C	Graphene content in PCM microcapsules	0.480	2	0.240	0.14	9.55
	Error	5.064	3	1.688		
	Sum	5.543	5			
−10 °C	Graphene content in the PCM microcapsules	0.149	2	0.075	0.04	9.55
	Error	4.995	3	1.665		
	Sum	5.145	5			

Table 7. Variance analysis of the stiffness results in the present SCB test.

Temperature	Source of Variance	Sum of Squares	Degrees of Freedom	Mean Square Error	F	F _{0.05}
−20 °C	Graphene content in PCM microcapsules	0.005	2	0.002	0.50	9.55
	Error	0.014	3	0.005		
	Sum	0.018	5			
−10 °C	Graphene content in the PCM microcapsules	0.005	2	0.002	0.50	9.55
	Error	0.014	3	0.005		
	Sum	0.018	5			

As seen in Tables 5–7, the F values of three test statistics in the present SCB tests were far below the critical value F_{0.05}. According to the variance analysis results, the content of CG in the phase-change microcapsule wall material shows no significant correlation with the present SCB test results.

3.1.2. Bending Test

(1) Test results

Next, the bending tests were performed on asphalt mixtures, using the method described in Section 2.2.2, during which the temperature was set at $-10\text{ }^{\circ}\text{C}$. Each specimen's bending strength, bending failure strain, bending stiffness modulus, and bending strain energy density were measured for evaluating the capability of resisting low-temperature shrinkage crack. The respective results are plotted in Figure 5.

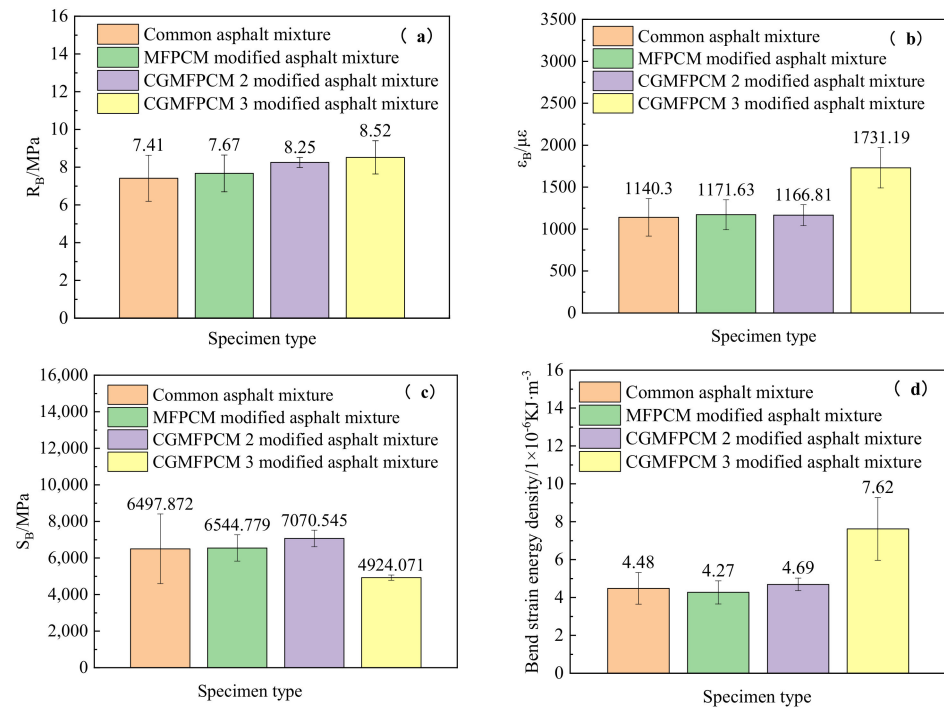


Figure 5. Bending test results for common and modified asphalt mixtures: (a) bending strength R_B , (b) bending failure strain ϵ_B , (c) bending stiffness modulus S_B and (d) bending strain energy density $\frac{dW}{dV}$.

As shown in Figure 5a, the beam bending strength of the asphalt mixture at $-10\text{ }^{\circ}\text{C}$ was enhanced after the addition of phase change microcapsules; moreover, the bending strength increased with the CG content. The beam bending test results at $-10\text{ }^{\circ}\text{C}$ confirmed the positive effect of adding CG on the material bending strength.

After adding phase-change microcapsules, the maximum tensile strain ratio of the beam, at the moment of beam bottom failure, was remarkably enhanced; in particular, the most significant enhancement was observed after adding CGMFPCM3. The tensile strain ratio, at the moment of beam bottom failure, can represent low-temperature deformability of the asphalt mixture, suggesting the enhancement of low-temperature crack resistance performance, after the addition of phase change microcapsules with a high mix ratio of CG. The CGMFPCM3-modified asphalt mixture showed a particularly good low-temperature performance.

As shown in Figure 5c, based on the temperature stress theory proposed by Hills [32], the bending stiffness modulus S_B , after the addition of MFPCM and CGMFPCM2, was slightly higher than that of the common asphalt mixture. Still, the respective value of the CGMFPCM3-modified asphalt mixture significantly decreased. Under the same cooling rate, thermal stresses that had accumulated in the asphalt mixture dropped significantly, thereby inhibiting the appearance of the low-temperature shrinkage cracking phenomenon.

Figure 5d shows the measured bending strain energy density values of common and modified asphalt mixtures. After the addition of MFPCM, the bending strain energy density of the asphalt mixture dropped slightly, while after adding CGMFPCM2, it was slightly enhanced. By contrast, the bending strain energy density of the CGMFPCM3-modified asphalt mixture exceeded that of the common asphalt mixture by 1.7 times.

Thus, the addition of CGMFPCM can enhance the crack resistance performance of the asphalt mixture; in particular, the CGMFPCM3-modified asphalt mixture showed the best resistance performance. Bending strain energy density can be regarded as a convenient and feasible index for evaluating the low-temperature performance of asphalt mixtures.

(2) Variance analysis

Tables 8–11 show the variance analysis and significance judgment results of the present bending test data.

Table 8. Variance analysis of the bending strength results in the performed beam bending tests.

Source of Variance	Sum of Squares	Degrees of Freedom	Mean Square Error	F	F _{0.05}
Graphene content in PCM microcapsules	1.893	2	0.947	1.33	4.10
Error	7.137	10	0.714		
Sum	9.030	12			

Table 9. Variance analysis of the bending failure strain results in the performed beam bending tests.

Source of Variance	Sum of Squares	Degrees of Freedom	Mean Square Error	F	F _{0.05}
Graphene content in PCM microcapsules	824,130.234	2	412,065.117	2.79	3.98
Error	1,624,549.828	11	147,686.348		
Sum	2,448,680.063	13			

Table 10. Variance analysis of the bending stiffness modulus results in the performed beam bending tests.

Source of Variance	Sum of Squares	Degrees of Freedom	Mean Square Error	F	F _{0.05}
Graphene content in PCM microcapsules	8,373,855.446	2	4,186,927.723	0.74	3.98
Error	62,298,028.765	11	5,663,457.160		
Sum	70,671,884.210	13			

Table 11. Variance analysis of the bending strain energy in the performed beam bending tests.

Source of Variance	Sum of Squares	Degrees of Freedom	Mean Square Error	F	F _{0.05}
Graphene content in PCM microcapsules	4.60309×10^{-11}	2	2.30154×10^{-11}	9.13	4.26
Error	2.26957×10^{-11}	9	2.52174×10^{-12}		
Sum	6.87266×10^{-11}	11			

Apparently, in terms of the F values, the bending strain energy density had the highest F value (9.13), followed by the bending failure strain ($F = 2.79$) and the bending strength ($F = 1.33$), while that of the bending stiffness modulus was the lowest ($F = 0.74$), suggesting that the content of CG in phase change microcapsule walls most significantly affected the bending strain energy density in the beam bending tests. Among four performance indices of the beam bending test, only the F value of the bending strain energy density of 9.13 exceeded the critical value of $F_{0.05} = 4.26$, as listed in Table 11. Variance analysis results imply that the content of graphene in the phase change microcapsule wall imposed the most significant effect on the bending strain energy density of the asphalt mixture but slightly affected its bending failure strain, bending strength, and bending stiffness modulus. Therefore, it is reasonable to adopt the bending strain energy density for evaluating the PCM-modified asphalt mixture's low-temperature performance.

3.2. Freeze–Thaw Splitting Tests

3.2.1. Test Results

The freeze–thaw splitting test results for the asphalt mixtures under study are tabulated in Table 12 and plotted in Figure 6.

Table 12. Freeze–thaw splitting test results for common and modified asphalt mixtures.

Specimen Type	RT ₂ /MPa	RT ₁ /MPa	TSR/%	
			Test Result	JTG F40
Common asphalt mixture	0.927	1.022	90.627	≥70
MFPCM-modified asphalt mixture	0.544	0.916	59.340	
CGMFPCM 2-modified asphalt mixture	0.660	0.822	80.307	≥75
CGMFPCM 3-modified asphalt mixture	0.787	0.859	91.647	

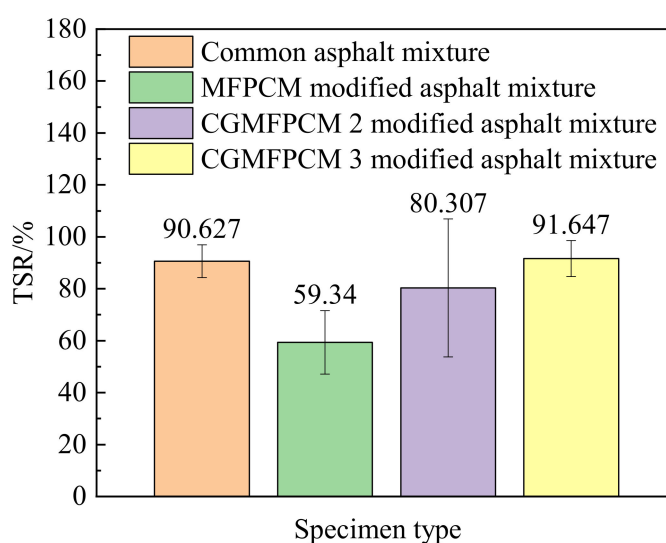


Figure 6. TSR results for common and modified asphalt mixtures in the performed freeze–thaw splitting tests.

As listed in Table 12, compared with the common asphalt mixture, the splitting tensile strength of all PCM-modified asphalt mixtures dropped due to water-induced damage, especially in the CGMFPCM3-modified asphalt mixture. It can be observed from Figure 5 that the tensile-to-strength ratio (TSR) of asphalt mixtures, after the addition of MFPCM and CGMFPCM2 in the freeze–thaw splitting tests, dropped to 59.34 and 80.303, respectively, as compared to that of the common mixture (90.627). The TSR ratio of the MFPCM-modified asphalt mixture failed to satisfy the requirements in the respective specifications (JTG F40); by contrast, the TSR ratio of the CGMFPCM3-modified asphalt mixture increased slightly (to 91.647). It can, thus, be concluded that the addition of MFPCM and CGMFPCM2 deteriorated the water stability of the asphalt mixture by 34.5 and 11.4%, respectively, while the addition of CGMFPCM3 only slightly improved the water stability of the asphalt mixture (by 1.1%). This is consistent with the results reported in the literature [20]. At the same time, it shows that the CG compound, in phase change microcapsules, is helpful to enhance the water stability of phase change modified asphalt.

3.2.2. Variance Analysis

Table 13 shows the variance analysis and significance judgment results of the present freeze–thaw splitting test data.

Table 13. Variance analysis of the bending strain energy in the performed freeze–thaw splitting test.

Source of Variance	Sum of Squares	Degrees of Freedom	Mean Square Error	F	F _{0.05}
Graphene content in PCM microcapsules	0.162	2	0.081	0.19	3.88
Error	5.085	12	0.424		
Sum	5.247	14			

As seen in Table 13, the F values of three test statistics in the present freeze–thaw splitting test were far below the critical value F_{0.05}. According to the variance analysis results, the content of CG in the phase-change microcapsule wall material shows no significant correlation with the present freeze–thaw splitting test results.

3.3. Wheel Tracking Test

3.3.1. Test Results

The wheel tracking test results for the asphalt mixtures under study are tabulated in Table 14 and plotted in Figure 6.

Table 14. Wheel tracking test results for common and modified asphalt mixtures.

Sample Name	Dynamic Stability/ Times·mm ⁻¹	JTG F40/Times·mm ⁻¹
Common asphalt mixture	2530	≥600
MFPCM-modified asphalt mixture	1270	≥1800
CGMFPCM 2-modified asphalt mixture	803	≥1800
CGMFPCM 3-modified asphalt mixture	2019	≥1800

According to Table 13 and Figure 7, in comparison with the asphalt mixture, the dynamic stability of all PCM-modified mixtures dropped, especially that of CGMFPCM3 (by about 68%). Since the specimens were kept at 60 °C for 5 h, the asphalt mixture fluidity could be enhanced by the phase change in PCMs, thereby increasing deformation and reducing dynamic stability under wheel pressure. As shown in Figure 7, after the addition of MFPCM and CGMFPCM2, the dynamic stability of the asphalt mixture dropped significantly (by about 50 and 68%), so the respective two mixtures failed to satisfy the requirements in JTG F40. By contrast, the CGMFPCM3-modified asphalt mixture, despite its reduced dynamic stability (by 20%), still satisfied the standard requirements.

3.3.2. Variance Analysis

Table 15 show the variance analysis and significance judgment results of the present wheel tracking test data.

Table 15. Variance analysis of the bending strain energy in the performed wheel tracking test.

Source of Variance	Sum of Squares	Degrees of Freedom	Mean Square Error	F	F _{0.05}
Graphene content in PCM microcapsules	1,933,268.019	2	966,634.010	1.06	5.14
Error	5,480,226.750	6	913,371.125		
Sum	7,413,494.769	8			

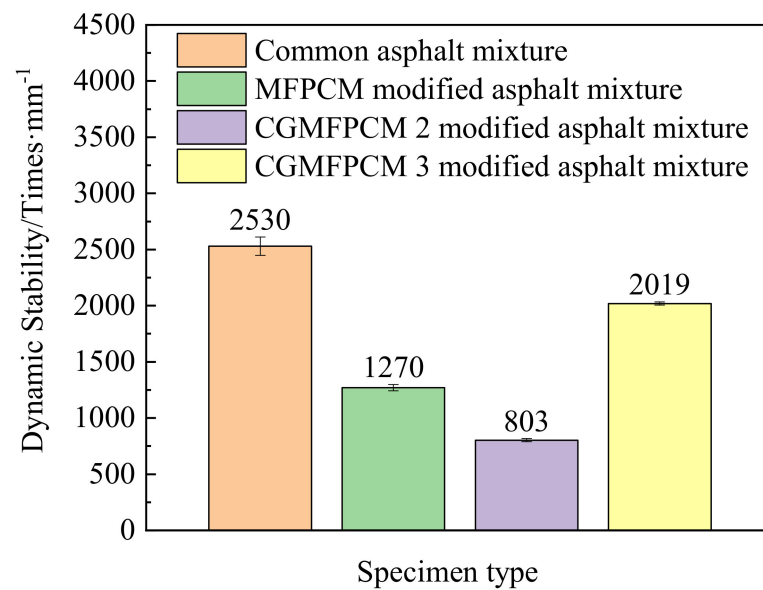


Figure 7. Wheel tracking test results of common and modified asphalt mixtures.

As seen in Table 15, the F values of three test statistics in the present wheel tracking test were far below the critical value $F_{0.05}$. According to the variance analysis results, the content of CG in the phase-change microcapsule wall material shows no significant correlation with the present wheel tracking test results.

3.4. Measurement of Thermal Conductivity and Heat Capacity of Asphalt Mixture

The test data on the thermal conductivity and volume-specific heat capacity of common and modified asphalt mixtures are plotted in Figures 8 and 9, respectively.

As shown in Figures 8 and 9, both thermal conductivities and volume-specific heat capacities of modified asphalt mixtures, within a temperature range from 268.15 to 298.15 K, exceeded the values of matrix asphalt. In particular, the MFPCM-modified asphalt mixture had the highest thermal conductivity, while the CGMFPCM3-modified asphalt mixture exhibited the largest volume-specific heat capacity. At 278.15 K, the thermal conductivity and volume-specific heat capacity of the asphalt mixture were enhanced by 5% and 43%, respectively, after the addition of CGMFPCM3, which confirmed that the temperature sensitivity of the asphalt mixture could be effectively reduced by adding phase-change modified materials.

The thermal conductivity and volume specific heat capacity of the ordinary asphalt mixture and modified asphalt mixture samples are linearly fitted, and the variation laws of thermal conductivity and volume specific heat capacity with temperature are shown in Tables 16 and 17, respectively. According to the analysis of variance (R^2), the errors of the fitting results are small. The change rate of the thermal conductivity of each sample has no significant relationship with CG content in phase change microcapsules, while the change rate of volume specific heat capacity has a significant relationship with CG content in phase change microcapsules. It increases significantly with the increase in CG content and is significantly higher than that of the ordinary asphalt mixture.

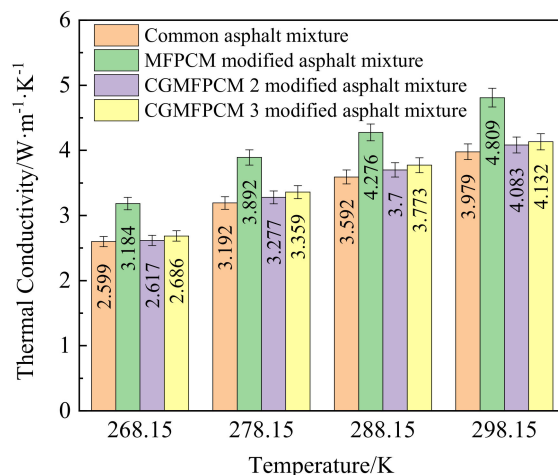


Figure 8. Thermal conductivity versus temperature curves of common and modified asphalt mixtures.

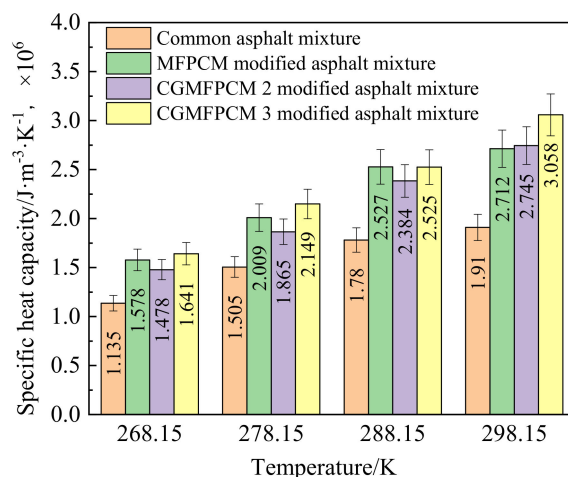


Figure 9. Measured volume-specific heat capacities of common and modified asphalt mixtures.

Table 16. Thermal Conductivity Rate of change of common and modified asphalt mixtures.

Sample Name	Thermal Conductivity Rate of Change/W·m ⁻¹ ·K ⁻²	R ²
Common asphalt mixture	0.0454	0.9883
MFPCM modified asphalt mixture	0.0526	0.9866
CGMFPCM 2 modified asphalt mixture	0.0482	0.9821
CGMFPCM 3 modified asphalt mixture	0.0475	0.9769

It is reported that the thermal conductivity of the modified asphalt mixture will decrease significantly with the increase in PCM content [50]. In this study, the CG compound in phase change microcapsules improves the heat conductivity of the modified asphalt mixture, which will help to give full play to the heat conduction and heat storage function of phase change microcapsules in the asphalt mixture. The comprehensive analysis of the overall experimental data revealed that the CGMFPCM3-modified asphalt mixture outperformed all others under study, in terms of low-temperature performance, water stability, high-temperature stability, and heat-conducting/storing performance.

Table 17. Volume specific heat capacity Rate of change of common and modified asphalt mixtures.

Sample Name	Volume Specific Heat Capacity Rate of Change/(J·m ⁻³ ·K ⁻² , ×10 ⁶)	R ²
Common asphalt mixture	0.026	0.9588
MFPCM modified asphalt mixture	0.0392	0.9658
CGMFPCM 2 modified asphalt mixture	0.0432	0.9953
CGMFPCM 3 modified asphalt mixture	0.0463	0.996

4. Material Cost Estimations

When phase change microcapsules are prepared by small-scale production in the laboratory, the preparation costs of phase-change microcapsules with different CG contents ranged from RMB 1491.44 to 3474.72 (USD 233.40 to 543.77) per kilo. Accordingly, the costs of prepared asphalt specimens, with a 5% content of phase-change microcapsules, increased by RMB 74.57~173.73 (USD 11.67~27.19) per kilo [43]. Based on this calculation, the cost added value of each ton of phase change microcapsule modified asphalt mixture (oil stone ratio is 5%) is between RMB 3728.59~8686.79 (USD 586.13~1365.56), as shown in Table 18.

Table 18. Preparation cost of phase change microcapsule modified asphalt mixture.

Type of Phase-Change Microcapsule	Preparation Cost per Ton of Phase Change Microcapsule Modified Asphalt Mixture, RMB/USD	
	Laboratory Preparation	Industrial Production
MFPCM	3728.59/586.13	45.24/7.11
CGMFPCM 2	7034.06/1105.75	96.09/15.11
CGMFPCM 3	8686.79/1365.56	121.52/19.10

Phase change microcapsules were prepared by industrial mass production, the preparation costs of phase-change microcapsules with different contents of CG could be eventually reduced to RMB 18.10~48.61 (USD 2.83 to 7.61), the modified asphalt specimens with 5% phase-change microcapsules increased by RMB 0.91~2.4 (USD 0.14 to 0.38) per kilo [43]. Based on this calculation, the cost added value of each ton of phase change microcapsule modified asphalt mixture (oil stone ratio is 5%) will be reduced to RMB 45.24~121.52 (USD 7.11~19.10).

5. Conclusions

The results obtained in this study made it possible to draw the following conclusions:

- (1) Among the indexes of bending test and semicircular bending performance test (SCB), the content of CG in the wall material of the phase change microcapsule is not significantly correlated with the results of the SCB test, but is significantly correlated with the results of bending strain energy density of the trabecular bending test. The bending strain energy density was found to be the most adequate index for evaluating the low-temperature performance of modified asphalt mixtures. With the increase in CG content in the wall material of the phase change microcapsule, the low-temperature crack resistance of the phase change temperature-regulating asphalt mixture is enhanced. The bending strain energy density of the CGMFPCM3-modified asphalt mixture exceeded that of the common asphalt mixture by 1.7 times, implying a better crack resistance performance of CGMFPCM3-modified asphalt.
- (2) Adding MFPCM and CFMFPCM2 deteriorated the water stability of the asphalt mixture by 34.5 and 11.4%, respectively, while the addition of CGMFPCM3 only slightly improved the water stability of the asphalt mixture (by 1.1%). Similarly, after the addition of MFPCM, CGMFPCM2, and CGMFPCM3, the dynamic stability of the asphalt mixture dropped by about 50, 68, and 20%. The latter mixture, despite its reduced dynamic stability, still satisfied the standard requirements.

- (3) Both thermal conductivity and volume-specific heat capacity can be used for evaluating the temperature-regulating performance of PCM-modified asphalt mixtures. All three PCM-modified asphalt mixtures outperformed common asphalt, in terms of thermal conductivity and volume-specific capacity. Specifically, the thermal conductivity of the MFPCM-modified asphalt mixture was the highest, while the CGMFPCM3-modified asphalt mixture had the largest volume-specific heat capacity. At 278.15 K, the thermal conductivity and volume-specific heat capacity of the latter mixture exceeded those of the common mixture by 5 and 43%, respectively. The thermal conductivity of the modified asphalt mixture had no significant difference with the change rate of the temperature, while the volume specific heat capacity had a great difference with the change rate of the temperature.
- (4) The modified asphalt mixture with the CGMFPCM3, synthesized by the authors, satisfied the technical requirements regarding water stability and high-temperature stability and exhibited excellent heat-conducting/storing capacity and low-temperature performance.

Author Contributions: Conceptualization, Y.-X.R.; Investigation, Y.-X.R.; Methodology, Y.-X.R.; Supervision, P.-W.H.; Validation, P.-W.H.; Writing—original draft, Y.-X.R. All authors have read and agreed to the published version of the manuscript.

Funding: Key Scientific Research Project of Higher Education of Henan Province (19A580002).

Institutional Review Board Statement: Not applicable.

Informed Consent Statement: Not applicable.

Data Availability Statement: All data, models, and codes generated or used in this study are included in the submitted manuscript.

Conflicts of Interest: The authors declare no conflict of interest.

References

1. Xu, S.F. Asphalt properties related to road performance. *J. Foreign Highw.* **1992**, *1*, 49–53.
2. Tan, Y.Q.; Bian, X.; Shan, L.Y.; Qu, L.Y.; Lu, J.F. Preparation of Latent Heat Materials Used in Asphalt Pavement and Its Performance of Temperature Control. *J. Build. Mater.* **2013**, *16*, 354–359.
3. Zhu, J.Y.; He, Z.Y.; Lin, F.F. Research on Anti-Icing Phase Change Asphalt Binder. *Mater. Rep.* **2015**, *29*, 472–475.
4. Kakar, M.R.; Refaa, Z.; Bueno, M.; Worlitschek, J.; Stamatiou, A.; Partl, M.N. Investigating Bitumen's Direct Interaction with Tetradecane as Potential Phase Change Material for Low Temperature Applications. *Road Mater. Pavement Des.* **2019**, *21*, 1–8. [[CrossRef](#)]
5. Chen, M.Z.; Wan, L.; Lin, J.T. Effect of Phase-Change Materials on Thermal and Mechanical Properties of Asphalt Mixtures. *J. Test. Eval.* **2012**, *40*, 746–753. [[CrossRef](#)]
6. Du, Y.F.; Liu, P.S.; Wang, J.C.; Wang, H.; Hu, S.W.; Tian, J.; Li, Y.T. Laboratory Investigation of Phase Change Effect of Polyethylene Glycol on Asphalt Binder and Mixture Performance. *Constr. Build. Mater.* **2019**, *212*, 1–9. [[CrossRef](#)]
7. Cao, C.B.; Luo, Y.M.; Li, W.H.; He, L.H.; Zhu, H.Z. Effect of Polyethylene Glycol on The Heat Storage Performance of Asphalt and Asphalt Mixture. *New Chem. Mater.* **2013**, *41*, 137–139.
8. Du, Y.F.; Liu, P.S.; Wang, J.C.; Dan, H.C.; Wu, H.; Li, Y.T. Effect of lightweight aggregate gradation on latent heat storage capacity of asphalt mixture for cooling asphalt pavement. *Constr. Build. Mater.* **2020**, *250*, 118849.
9. Zhou, X.Y.; Ma, B.; Ren, Y.Z.; Wang, X.Q. Study on temperature regulation effect of composite shape stabilized phase change materials for asphalt pavement. *Silic. Bull.* **2018**, *37*, 3611–3616.
10. Huang, W. *Small-Scale Preparation and Properties of Epoxy Resin Composite Phase Change Thermostat*; Chang'an University: Xi'an, China, 2017.
11. Chang, X.Y. *Experimental Study on Temperature Control Effect of Epoxy Resin Compound Temperature Control Agent and Specific Heat Capacity of Asphalt Mixture*; Chang'an University: Xi'an, China, 2017.
12. Ma, X.; Xiao, Y.; Zhang, W.J.; Yu, M. Study on the basic properties of epoxy resin composite phase change materials. *Bull. Chin. Ceram. Soc.* **2018**, *37*, 2536–2542.
13. Cho, J.S.; Kwon, A.; Cho, C.G. Microencapsulation of octadecane as a phase-change material by interfacial polymerization in an emulsion system. *Colloid Polym. Sci.* **2002**, *280*, 260–266. [[CrossRef](#)]
14. Wang, Z.J.; Wang, X.L.; Xiang, H. Research on the temperature regulation performance of a kind of constant temperature asphalt concrete. *J. China Foreign Highw.* **2015**, *35*, 268–272.

15. Li, X. Effect of phase change temperature regulating materials on high temperature performance and temperature control performance of asphalt and asphalt mixture. *New Chem. Mater.* **2019**, *47*, 253–256, 263.
16. Wang, Y.C. *Preparation of Tetradecane/Melamine Formaldehyde Resin Phase Change Microcapsules and Properties of Modified Asphalt*; Chang'an University: Xi'an, China, 2017.
17. Wei, K.; Wang, Y.C.; Ma, B. Effects of microencapsulated phase change materials on the performance of asphalt binders. *Renew. Energy* **2019**, *132*, 931–940. [[CrossRef](#)]
18. Ye, S.H. *Preparation of Phase Change Microcapsules and Its Application in Asphalt*; Harbin Institute of Technology: Harbin, China, 2018.
19. Li, F.; Zhou, S.Q.; Chen, S.; Yang, J.; Zhu, X.Y.; Du, Y.C.; Yang, Z.L. Low-temperature organic phase change material microcapsules for asphalt pavement: Preparation, characterisation and application. *J. Microencapsul.* **2018**, *35*, 635–642. [[CrossRef](#)]
20. Li, F.; Zhou, S.Q.; Chen, S.; Yang, Z.L.; Yang, J.; Zhu, X.Y.; Du, Y.C.; Zhou, P.T.; Chen, Z.H. Preparation of Low-Temperature Phase Change Materials Microcapsules and Its Application to Asphalt Pavement. *J. Mater. Civ. Eng.* **2018**, *30*, 04018303. [[CrossRef](#)]
21. Kakar, M.R.; Refaa, Z.; Worlitschek, J.; Stamatiou, A.; Partl, M.N.; Bueno, M. Thermal and rheological characterization of bitumen modified with microencapsulated phase change materials. *Constr. Build. Mater.* **2019**, *215*, 171–179. [[CrossRef](#)]
22. Kakar, M.R.; Refaa, Z.; Worlitschek, J.; Stamatiou, A.; Partl, M.N.; Bueno, M. Effects of aging on asphalt binders modified with microencapsulated phase change material. *Compos. Part B Eng.* **2019**, *173*, 107007. [[CrossRef](#)]
23. Bueno, M.; Kakar, M.R.; Refaa, Z.; Worlitschek, J.; Stamatiou, A.; Partl, M.N. Modification of asphalt mixtures for cold regions using microencapsulated phase change materials. *Sci. Rep.* **2020**, *9*, 20342. [[CrossRef](#)]
24. Phan, T.M.; Park, D.W.; Le, T.H.M. Improvement on rheological property of asphalt binder using synthesized micro-encapsulation phase change material. *Constr. Build. Mater.* **2021**, *287*, 123021. [[CrossRef](#)]
25. ASTM D7313-13; Standard Test Method for Determining Fracture Energy of Asphalt-Aggregate Mixtures Using the Disk-Shaped Compact Tension Geometry. ASTM International: West Conshohocken, PA, USA, 2013. [[CrossRef](#)]
26. American Association of State Highway and Transportation Officials (AASHTO). *Standard Method of Test for Determining the Creep Compliance and Strength of Hot Mix Asphalt (HMA) Using the Indirect Tensile Test Device*; T 322; AASHTO: Washington, DC, USA, 2007.
27. American Association of State Highway and Transportation Officials (AASHTO). *Standard Method of Test for Determining the Fracture Energy of Asphalt Mixtures Using the Semicircular Bend Geometry (SCB)*; TP 105; AASHTO: Washington, DC, USA, 2019.
28. EN 12697-44; Bituminous Mixtures—Test Methods—Part 44: Crack Propagation by Semi-Circular Bending Test. Comité Européen de Normalisation(CEN): Brussels, Belgium, 2019.
29. American Association of State Highway and Transportation Officials (AASHTO). *Standard Test Method for Thermal Stress Restrained Specimen Tensile Strength*; TP10; AASHTO: Washington, DC, USA, 1993.
30. GB/T 38948; Evaluation Method for the Cracking Resistance of Asphalt Mixture at Low Temperatures. China Standard Press: Beijing, China, 2020.
31. Feng, D.C.; Cui, S.T.; Yi, J.Y.; Chen, Z.G.; Qin, W.J. Research on Evaluation Index of Low Temperature Performance of Asphalt Mixture Based on SCB Test. *China J. Highw. Transp.* **2020**, *33*, 50–57.
32. Hills, J.F. *Predicting the Fracture of Asphalt Mixes by Thermal Stresses*; Institute of Petroleum: London, UK, 1974.
33. Ren, J.P. *Analysis on Influence of Micro-Encapsulated Phase Change Thermoregulation Agent on Temperature Field of Asphalt Pavement*; Chang'an University: Xi'an, China, 2015.
34. Wang, H. *Study on Properties and Temperature-regulating Mechanism of PEG/SiO₂ Composite Phase Change Heat Storage Asphalt Mortar*; Chongqing Jiaotong University: Chongqing, China, 2019.
35. Tan, H.Q. Study on the temperature adjustment effect and road performance of phase change asphalt mixture. *Hunan Transp. Sci. Technol.* **2021**, *47*, 40–43.
36. Wang, X.Q.; Ma, B.; Liu, F.W. Study on Temperature Field of Microcapsule Phase Change the Thermostatic Asphalt Mixture. *J. Wuhan Univ. Technol.* **2020**, *44*, 1020–1026.
37. Dong, S.X. *Study on Preparation and Properties of Mixture at Micro-Surface of Phase Change Temperature Control*; College of Civil Engineering: Handan, China, 2020.
38. Wei, K.; Wang, X.Q.; Ma, B.; Shi, W.S.; Duan, S.Y.; Liu, F.S. Study on rheological properties and phase-change temperature control of asphalt modified by polyurethane solid–solid phase change material. *Sol. Energy* **2019**, *194*, 893–902. [[CrossRef](#)]
39. Liu, X.Y. *Preparation of Phase Change Microcapsules for Snow Melting and Research on Performance of Phase Change Asphalt and Mixture*; Harbin Institute of Technology: Harbin, China, 2020.
40. Athukorallage, B.; Dissanayaka, T.; Senadheera, S.; James, D. Performance analysis of incorporating phase change materials in asphalt concrete pavements. *Constr. Build. Mater.* **2018**, *164*, 419–432. [[CrossRef](#)]
41. Zhou, X.X.; Zhang, X.; Xu, S.; Wu, S.P.; Liu, Q.T.; Fan, Z.P. Evaluation of Thermo-mechanical Properties of Graphene/Carbon-nanotubes Modified Asphalt with Molecular Simulation. *Mol. Simul.* **2017**, *43*, 312–319. [[CrossRef](#)]
42. Yao, H.; Dai, Q.L.; You, Z.P.; Bick, A.; Wang, M. Modulus Simulation of Asphalt Binder Models Using Molecular Dynamics (MD) Method. *Constr. Build. Mater.* **2018**, *162*, 430–441. [[CrossRef](#)]
43. Ren, Y.X.; Hao, P.W. Modification mechanism and enhanced low-temperature performance of asphalt mixtures with graphene-modified phase-change microcapsules. *Constr. Build. Mater.* **2022**, *320*, 126301. [[CrossRef](#)]
44. Ren, Y.X.; Hao, P.W.; Zhao, C.Z.; Wu, T.; Li, D.W. Study on compatibility and enhancement mechanism of phase change microcapsules with asphalt based on molecular dynamics. *China J. Highw. Transp.* **2020**, *33*, 178–191.

45. *JTG F40-2004*; Technical Specification for Construction of Highway Asphalt Pavements. China Communication Press: Beijing, China, 2004.
46. *T0702-2011*; Preparation Method of Asphalt Mixture Specimen (Compaction Method). China Communication Press: Beijing, China, 2011.
47. *T0715-2011*; Asphalt Mixture Bending Test. China Communication Press: Beijing, China, 2011.
48. *T0729-2000*; Freeze Thaw Splitting Test of Asphalt Mixture. China Communication Press: Beijing, China, 2011.
49. *T0703-2011*; Preparation Method of Asphalt Mixture Specimen (Wheel Rolling Method). China Communication Press: Beijing, China, 2011.
50. Cheng, C.; Gong, F.Y.; Fu, Y.R.; Liu, J.; Qiao, J.G. Effect of polyethylene glycol/polyacrylamide graft copolymerization phase change materials on the performance of asphalt mixture for road engineering. *J. Mater. Res. Technol.* **2021**, *50*, 1970–1983. [[CrossRef](#)]